



# Chitosan-based coatings for corrosion protection of copper-based alloys: A promising more sustainable approach for cultural heritage applications

Chiara Giuliani<sup>a,\*</sup>, Marianna Pascucci<sup>a</sup>, Cristina Riccucci<sup>a</sup>, Elena Messina<sup>a</sup>,  
Martina Salzano de Luna<sup>b</sup>, Marino Lavorgna<sup>b</sup>, Gabriel Maria Ingo<sup>a</sup>, Gabriella Di Carlo<sup>a,\*</sup>

<sup>a</sup> Institute for the Study of Nanostructured Materials, National Research Council (ISMN-CNR), Via Salaria km 29,300, 00015 Monterotondo, RM, Italy

<sup>b</sup> Institute of Polymers, Composites and Biomaterials, National Research Council (IPCB-CNR), Piazzale Fermi 1, 80055 Portici, NA, Italy

## ARTICLE INFO

### Keywords:

Sustainable coating  
Chitosan  
Active protection  
Corrosion inhibitors  
Bronze

## ABSTRACT

The attractive physicochemical properties of chitosan make its derived materials promising candidates for the reliable and sustainable corrosion protection of metallic substrates. In this work, chitosan-based coatings embedding different corrosion inhibitors, i.e. benzotriazole (BTA) and mercaptobenzothiazole (MBT), were investigated for the protection of copper-based alloys, with the aim to extend their application to the preservation of works of art exposed to indoor atmosphere. The composition of the formulations was optimized paying particular attention to their potential application in the field of cultural heritage. To assess the efficacy of the coatings, tailored accelerated corrosion tests were carried out on bare and coated bronze substrates. Coated and uncoated alloy disks were characterized before and after corrosion treatments by optical microscopy, scanning electron microscopy, energy-dispersive X-ray spectroscopy and Fourier transform infrared spectroscopy. Moreover, an image analysis protocol was defined to evaluate the extent of surface modifications after degradation treatments. The obtained results revealed that the chitosan-based coatings containing BTA and MBT fulfil the aesthetic criteria required in the field of cultural heritage and are able to inhibit the corrosion of bronze alloys. It is worth noting that a synergic effect between the chemical protection provided by the inhibitors and the physical one provided by the polymer matrix was observed. Our findings demonstrate that the developed systems are suitable for a reliable and more sustainable protection of indoor bronze artefacts, thus representing a promising alternative to commercial products and particularly taking advantage from the use of non-harmful solvents for their application and removal.

## 1. Introduction

The development of high-performance materials that satisfy requirements related to environmental sustainability and cost-effectiveness represents a serious challenge for the scientific community. Specifically, in the field of art conservation the research of effective and non-toxic corrosion protective treatments has recently registered a significant increase, due to new strict health and safety regulations related to the use of chemical products, as well as to the need of reducing the use of petroleum-derived materials [1].

A valid strategy for the protection of metal substrates is the use of “active” coatings consisting of a passive polymer matrix loaded with chemically active compounds, such as corrosion inhibitors.

Differently from the direct application of corrosion inhibitors on the metal surface, which is one of the currently used procedure [2], their incorporation into the polymer matrix may provide a twofold

advantage: (i) it allows to use low amount of inhibitors; and (ii) it permits to immobilize them in the coating, thus possibly reducing their leaching in the environment and obtaining long-lasting protective films. Note that the most commonly used corrosion inhibitors for copper and copper-based alloys, such as benzotriazole (BTA) and its derivatives [3], are toxic (as pure inhibitor) and this aspect represents a critical issue for what concerns their handling and leaching in the environment [4,5].

In this scenario, the use of eco-friendly polymeric materials obtained from renewable sources, which act both as barrier layer and reservoir for corrosion inhibitors, is an attractive approach for the development of reliable, sustainable and active protective coatings [6–11]. The choice of natural polymers that are soluble in water-based solutions may avoid the use of harmful solvents (as toluene, acetone, white spirit and xylene) that are necessary for the application and removal of commonly used commercial protective coatings, consisting of

\* Corresponding authors.

E-mail addresses: [chiara.giuliani@ismn.cnr.it](mailto:chiara.giuliani@ismn.cnr.it) (C. Giuliani), [gabriella.dicarlo@ismn.cnr.it](mailto:gabriella.dicarlo@ismn.cnr.it) (G. Di Carlo).

BTA dispersed in acrylic resins (Paraloid B72™, 70 methylmethacrylate/30 ethyl acrylate copolymer) or microcrystalline waxes [2]. Therefore the development of innovative water-soluble products is mandatory, especially for conservation interventions on unmovable works of art.

It is also worth noting that “ideal” protective coatings for cultural heritage applications, besides preventing substrate degradation by using safe procedures, have to fulfil demanding aesthetic requirements. In particular, they have to be transparent and colourless, avoiding any modification in the appearance of the works of art, and they have also to be easily applicable and removable.

In the field of polymer-based coatings, chitosan turned out to be a very interesting material and a good alternative to conventional coating systems due to its intrinsic properties, including biocompatibility, antimicrobial activity, biodegradability, superior adhesion to metallic surfaces and the ability to reversibly form complexes with potential corrosion inhibitors [12,13]. Moreover, chitosan is soluble in aqueous media and can be obtained from renewable sources. It derives from the partial deacetylation of chitin, which is the main constituent of the exoskeleton of crustaceans and insects and it is one of the most abundant biopolymer in nature. The structure of chitosan, consisting of  $\beta$ -(1–4)-2-acetamido-D-glucose and  $\beta$ -(1–4)-2-amino-D-glucose units, also gives to the polymer excellent film forming ability, which makes it suitable for applications in various fields [14–17]. The interest in chitosan as a coating for metallic substrates has increased in recent years, especially for magnesium [18–20] and steel alloys [21] used for biomedical applications. The development of chitosan coatings doped with  $\text{Ce}^{3+}$  metal cations or containing 2-mercaptobenzothiazole (MBT) as corrosion inhibitors have been previously reported in literature also for the protection of aluminium alloys [22,23]. Moreover, chitosan-based low-pH-sensitive hydrogels loaded with BTA were prepared by Li et al. [3]. They investigated BTA loading capacity and releasing ability of the hydrogels and their performance in the corrosion protection of copper. Little has been reported about chitosan as green inhibitor for copper corrosion in acidic medium [24] and studies reporting the use of chitosan for copper-based alloys in the field of cultural heritage are scarce.

In the present work, active coatings based on chitosan with two different corrosion inhibitors, BTA and MBT, as sustainable and water-soluble corrosion protective systems for the conservation of indoor bronze artefacts were investigated. A copper-based alloy, with chemical composition and metallurgical features similar to those commonly used in bronze objects of art, was used as the metallic substrate. The BTA was selected since it is the most commonly used corrosion inhibitor, whereas MBT is considered a promising low toxic alternative [23,25–28]. The effect of the type of acid used for chitosan dissolution, i.e. acetic acid (AcOH) and D-(+)-Gluconic  $\delta$ -lactone (GDL), on the quality of the films deposited onto the bronze substrates and on the interaction of the polymer with the metal alloy was studied. The influence of glycerol addition, as plasticizer, on the morphological and protective properties of the coatings was also evaluated. Optical microscopy and scanning electron microscopy (SEM) were employed to evaluate the coating morphology and micro-structure. Fourier transform infrared spectroscopy (FTIR) and energy-dispersive X-ray spectroscopy (EDS) were used to investigate the coating/substrate interaction and to get information about the surface chemical composition. To assess the protective efficacy, tailored accelerated corrosion tests were optimized starting from a procedure previously reported in literature [29]. They consist of a mild heating of the bare and coated bronze substrates in the presence of acidic water vapours, which represent a more realistic environment with respect to the commonly used immersion in acidic solutions. The coated disks and the bare alloy used as reference were characterized by optical microscopy, SEM, EDS and FTIR before and after the accelerated corrosion treatments. An image analysis protocol was also defined to evaluate the extent of surface modifications after degradation tests. To the best of our knowledge, the

active protection of bronze alloys by using chitosan-based coatings for the preservation of indoor works of art and their assessment with tailored procedures have not been reported so far.

## 2. Materials and methods

### 2.1. Materials

Chitosan (medium molecular weight, viscosity 200–800 cP, 75–85% deacetylated), D-(+)-gluconic  $\delta$ -lactone (purity  $\geq 99.9\%$ ), 2-mercaptobenzothiazole (purity 98%) and glycerol (analytical grade) were purchased from Sigma Aldrich. Benzotriazole (purity 99%) was purchased from Bresciani. Glacial acetic acid (purity 99.9%) was purchased from Carlo Erba, ethanol (EtOH, purity  $\geq 99.8\%$ ) and water Cromasolv plus for HPLC were purchased from Sigma Aldrich. Before using, chitosan was washed in boiling water for 1 h, filtered, thoroughly washed with distilled water to remove impurities, and dried under vacuum for 12 h. A bronze alloy, with commonly used chemical composition [30,31] was purposely produced (labelled CNR 128, nominal composition of 92.8% Cu, 6.8% Sn, 0.2% Pb) and was used as the metallic substrate. The alloy disks have been polished by using SiC papers at 1200 grit and diamond pastes up to 1/4  $\mu\text{m}$  in order to obtain a flat and smooth surface with a mirror-like finish. After polishing, the Cu-based alloys have been cleaned with ethanol.

### 2.2. Preparation of chitosan-based solutions and coatings

Chitosan solutions were prepared by dissolving 0.5 wt/vol% of purified chitosan in aqueous 0.1 M AcOH solution or in 0.05 M GDL solution. The concentrations of the two acids was selected in order to obtain a solution with a pH  $\sim 3.5$ . The initial dispersions were stirred for 24 h at 30 °C to achieve total dissolution of chitosan. The pH of the solutions was then adjusted to 6 by the addition of 1 M NaOH. The corrosion inhibitor, BTA or MBT (0.1 wt.% with respect to chitosan solution), was added to aqueous chitosan solutions with either AcOH or GDL. Glycerol (4 wt.% with respect to chitosan solution) was also used in some formulations. All the solutions were diluted with EtOH to obtain a mixture with a final water/ethanol ( $\text{H}_2\text{O}/\text{EtOH}$ ) composition of 50/50 v%/v%. Therefore, the final inhibitor concentration in the water/ethanol formulation was 0.05 wt/vol%.

All the coatings were prepared by drop-casting 60  $\mu\text{L}$  of the  $\text{H}_2\text{O}/\text{EtOH}$  chitosan-based solutions or 30  $\mu\text{L}$  of only inhibitor solution (0.1 wt/vol% in ethanol) onto bronze disks with a diameter of 2.5 cm and by subsequent drying at room temperature. Removability tests were carried by using tissue paper soaked in water or ethanol.

### 2.3. Determination of the bronze disk wettability

Contact angle measurements were performed to determine the optimal composition of the liquid phase of the coating formulations and to quantitatively evaluate their wettability on the bronze substrates. The static contact angle ( $\theta$ ) was estimated with an automatic video-based measurement of contact angle performed at room temperature and humidity by using a Dataphysics OCA-20 Contact Angle System. Five microliters of liquid were placed on the bronze substrate and the Young/Laplace method has been used to calculate the static contact angle. Fifteen independent measurements were carried out for each type of liquid investigated to take into account the variability due to the surface roughness of the bronze disks. In addition, every five measurements the substrate was subjected to the polishing procedure. In such a way, the reproducibility of the polishing step was also verified.

### 2.4. Measurements of film thickness

The thickness of the deposited coatings was estimated by using a nanoindentation equipment (Nanotest Platform 2, Micromaterials) in

scanning mode. First, a portion of the coating was gently removed from the bronze disk using water, in order not to alter the characteristics of the substrate surface. Then, the depth reached by the nanoindenter tip was monitored along a path of about 5 mm over the area with and without the coating. The difference of the reached depth between such two areas was taken as representative of the coating thickness. Note that preliminary tests were performed to choose the applied probing load (0.1 mN) in order not to deform the coating while measuring.

## 2.5. Transparency measurements

The transparency of chitosan coatings was measured by depositing the different formulations on glass slides (same thickness of coatings on bronze disks) and then measuring the percentage of transmitted light in the visible range of wavelengths from about 390–700 nm, by using an UV–vis spectrophotometer. An uncovered glass slide was used as reference for 100% of transmittance.

## 2.6. Micro-chemical, morphological and structural analysis by SEM–EDS, OM and FTIR

All bare and coated bronze disks were characterized before and after corrosion tests. Micro-chemical and –morphological characterisations were performed by means of a scanning electron microscope (SEM) Cambridge 360 equipped with a LaB6 filament and a high brilliance LEO 1530 field emission scanning electron microscope (FE-SEM) apparatus equipped with an energy dispersive X-ray spectrometer (EDS) INCA 250 and INCA 450, respectively, and a four sector back-scattered electron (BSE) and secondary electron (SEI) detectors. Optical microscopy (OM) investigations were performed by using a Leica MZFLIII microscope equipped with a digital camera (Leica DFC 320).

Bronze disks coated with chitosan-based films and Pb disks coated with chitosan, AcOH and GDL as control samples were characterized by Attenuated Total Reflectance Fourier Transform Infrared (ATR-FTIR) spectroscopy. The spectra were collected using a Nicolet iS50 spectrometer (Thermo Fisher) equipped with an ATR accessory. The measurements were recorded using a diamond crystal cell ATR using typically 32 scans at a resolution of  $4\text{ cm}^{-1}$ . The samples were all measured under the same mechanical force pushing the samples in contact with the diamond crystal. No ATR correction has been applied to the data.

## 2.7. Accelerated corrosion test

Accelerated corrosion tests were carried out by heating bare and coated bronze disks into a closed glass vessel at  $50\text{ }^\circ\text{C}$  for 1 h in presence of acid vapours. Note that bronze disks were put into the closed vessel in the presence of an aqueous HCl solution 1 M, but not in direct contact with it [29,30].

Image analysis was exploited to observe modifications occurring at the metal surface after accelerated corrosion tests at different time intervals (up to 3 h). Optical images were collected to investigate the alloy surface without removing the coatings, thus observing only modification induced by degradation treatments. The image analysis was carried out on the bare alloy disks and on the disks covered with chitosan-based coating containing BTA or MBT as corrosion inhibitors to estimate the average corroded surface area. The description of the image processing procedure is reported in the Supporting Information (Fig. S1).

## 3. Results and discussion

### 3.1. Optimization of chitosan coatings

Chitosan is insoluble in most organic solvents, but readily soluble in dilute aqueous acids at pH below 6 [32] because of the protonation of its free primary amino groups [33]. They are regarded as a strong base

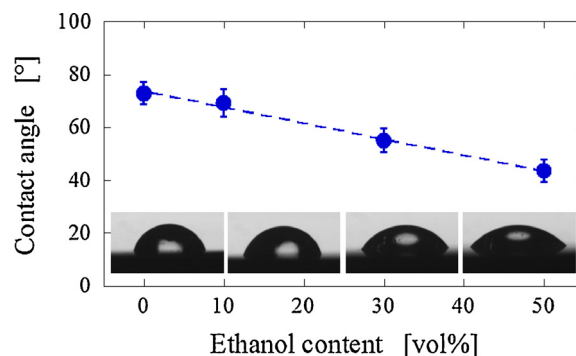


Fig. 1. Contact angle values on the polished bronze substrate of (a) water/ethanol mixtures at different ethanol content.

with a pKa value of 6.3 [34], thus under this pH value they are protonated and positively charged which lead chitosan as a cationic water-soluble polyelectrolyte. Among various inorganic and organic acids that can dissolve chitosan in aqueous solution [35–37], the acidifying agents selected for our study are AcOH, the most commonly used, and GDL, for a gradual pH decrease. The strong inorganic HCl, as well as other chloride based acids, were avoided since it is well known that chloride ions promote corrosion processes in copper based alloys [30,38–40]. After polymer dissolution, the pH of the solution was increased up to 6 in order to avoid the corrosion of bronze surface, catalysed by acidic species. Anyway, the final pH value should not exceed 6 to prevent the deprotonation of chitosan's amines, which causes the polymer to lose its charge, precipitating. According with a set of safety, health and environmental criteria recommended in literature [41], the water/ethanol mixture was selected as final liquid medium of the coating formulations and preliminary wettability analyses were performed to optimize the composition of the solvent mixture. Specifically, the contact angle on the bronze disks of water and water/ethanol mixtures at different composition was investigated.

From the data in Fig. 1, it clearly emerges that the addition of ethanol substantially influences the wetting behaviour of the liquid drops on the bronze substrate. Specifically, the contact angle value decreases almost linearly by increasing the ethanol content (Fig. 1). For the chitosan solutions prepared with different acids, no differences were observed in the wetting behaviour (Fig. S2). Such a result suggests that the contact angle of the coating formulations on the bronze disks is essentially governed by the solvent mixture.

From a practical perspective, the water/ethanol composition that ensures both the lowest contact angle and the complete dissolution of the polymer has to be preferred. In the light of this consideration, the water/ethanol mixture at the composition of 50/50 v%/v% was selected as liquid medium for the chitosan formulations. Note that mixtures containing higher contents of ethanol were not considered in the analysis because they are responsible for a decrease of chitosan solubility.

Optical images of the alloy disks coated with chitosan films are shown in Fig. 2 and the bare CNR128 alloy disk is reported as reference. The chitosan film from GDL solution appears colourless, more transparent and uniform than that prepared from AcOH solution, and it satisfies the aesthetic requirements for application in cultural heritage. Differently from the commonly used AcOH, the GDL acidifying agent acts dissolving chitosan by a gradual decrease of the pH value. In fact, when the GDL is brought into contact with water, its hydrolysis to gluconic acid slowly occurs, thus resulting in a gradual shift of the solution pH in the acidic region [42,43]. The decrease of pH is responsible for the protonation of chitosan amino groups and hence for its gradual charging and dissolution. The possibility of getting a slow dissolution of chitosan through the use of GDL could contribute to the formation of a more homogeneous and stable dispersion of the

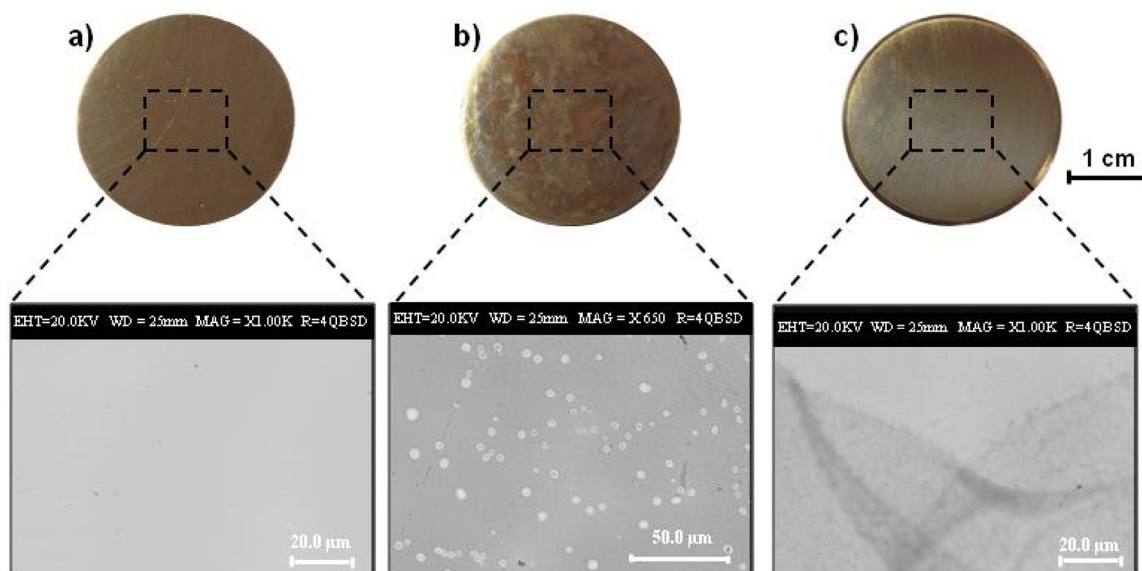


Fig. 2. Photographs and SEM images of (a) bare CNR128 alloy disk, and disks coated with chitosan film prepared from (b) AcOH and (c) GDL solutions.

biopolymer, which likely gives rise to high quality films [42].

The role of the acidifying agent on the coating/substrate interaction was thoroughly investigated. In particular, SEM analyses of CNR 128 alloy coated with chitosan film from AcOH reveal the presence of many platelets on the disk surface and within the polymeric coating (Fig. 2), thus pointing out the possible different interaction between the acidifying agents and the alloy substrate. As shown in Fig. 3, the EDS spectra reveal a significantly high Pb percentage in the platelets.

In order to get more information about their formation, chitosan films from AcOH were deposited onto Cu-based alloys without Pb. SEM analysis revealed the absence of platelets (data not shown), thus further confirming that their formation is strictly related to the interaction of the film with Pb. It is worth noting that SEM analyses of CNR 128 alloy coated with chitosan from GDL solutions (Fig. 2) do not reveal the presence of platelets and this could be responsible for the observed better quality and transparency of these films.

The role of the acidifying agent in the film interaction with Pb was also investigated by depositing three different aqueous solutions containing (i) only AcOH, (ii) only GDL and (iii) chitosan dissolved using HCl (that is without either AcOH or GDL) onto Pb disks. HCl and GDL solution does not affect the Pb appearance, on the contrary the deposition of AcOH solution leads to the formation of a white patina (Fig. S3), thus suggesting the formation of Pb acetate species. The Pb disks coated with AcOH, GDL and chitosan prepared from HCl were also investigated by FT-IR analysis (Fig. 4) and absorption bands around  $1400$ ,  $850$  and  $700\text{ cm}^{-1}$ , attributed to the asymmetric stretching

vibration and to in-plane and out-plane bending vibration of carboxylate groups [44], were detected only in the spectrum a of Pb disk coated with AcOH solution. These data support the hypothesis that platelets mainly consist of Pb-acetate species. In the other two spectra, only typical peaks of GDL and chitosan can be observed according to data reported in literature [23].

Based on these preliminary investigations, GDL was selected as acidifying agents for the dissolution of chitosan, and the mixture water/ethanol 50/50 as final liquid medium for the coating formulations. The concentration of the polymer and the volume of the solution deposited on the alloy disks was optimized to prepare thin film with a thickness of about 200–250 nm.

### 3.2. Effect of the addition of different corrosion inhibitors and glycerol to chitosan film

With the aim of developing chitosan-based coating for the active corrosion protection of bronze substrates, different corrosion inhibitors, namely BTA and MBT, were incorporated into the polymer matrix. Their concentration was optimized to ensure the good appearance and anticorrosion properties of the coatings and to minimize the amount of inhibitor. It was observed that the addition of BTA leads to transparent, uniform and cracks-free films (Fig. 5a). The addition of MBT does not affect the transparency of chitosan films but SEM analyses put in evidence the presence of micrometric needle-shaped crystals, as shown in Fig. 5b. EDS analysis on these crystals, with a high percentage of

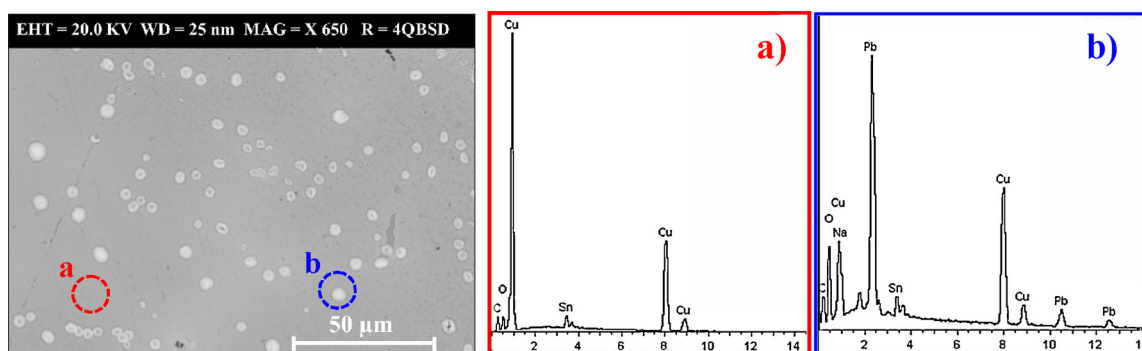


Fig. 3. SEM image and EDS analyses of chitosan films prepared from AcOH solutions deposited on alloy CNR128 substrate. The EDS spectra refer to the areas marked as “a” and “b” in the SEM micrograph.



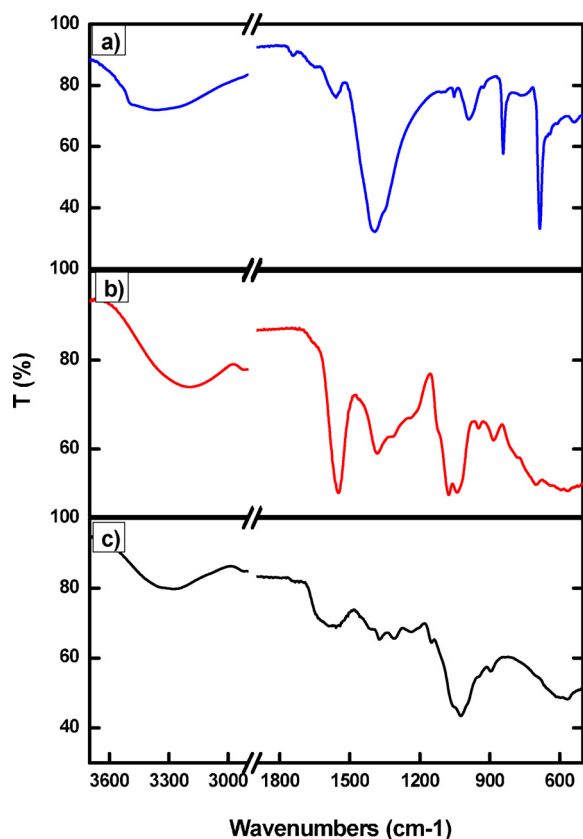


Fig. 4. FTIR spectra of Pb disks coated with an aqueous solution of diluted a) AcOH, b) GDL and c) chitosan film prepared by HCl.

sulphur, support the hypothesis that they mainly consist of corrosion inhibitor (Fig. S4). It is important to consider that even in the presence of MBT crystals, the coating maintains a percentage of transparency higher than 98% in all the visible range (Fig. 5c). The needle-like crystals formation may be due to the poor solubility of MBT in water. It is not possible to get further information on the MBT/chitosan interaction by FTIR spectroscopy because of the low amount of MBT trapped within the chitosan matrix. However, some degree of chemical interaction cannot be entirely discarded. Considering the presence of protonated amine and hydroxyl groups on chitosan, as well as nitrogen and thiol functionalities on MBT, hydrogen bonding, ion-dipole and dipole-dipole interactions may occur.

According to the literature [19], some properties of chitosan-based films are usually improved by the addition of plasticizing agents, which increases film pliability and flexibility by interfering with the hydrogen bonding between chitosan macromolecules. Based on these considerations, chitosan formulation from GDL containing glycerol and both

glycerol and BTA were also investigated with the aim to combine the positive effect of the plasticizer on film quality and the anticorrosion properties of the inhibitor on bronze. The addition of glycerol to the chitosan/BTA formulation from GDL preserves the good quality of the film, thus leading to the formation of a transparent and uniform film.

### 3.3. Anticorrosion properties of chitosan-based films

To evaluate the efficacy of the coatings, accelerated corrosion tests were carried out on bare and coated bronze disks in the presence of acidic water vapours, reproducing in a quite realistic way the actual ageing environment. The coated disks and the bare alloy used as reference were characterized by optical microscopy, SEM, EDS and ATR-FTIR before and after the accelerated corrosion treatments. Different chitosan formulations were used: pure chitosan, chitosan/glycerol, chitosan/BTA, chitosan/MBT chitosan/glycerol/BTA all prepared from GDL. In Fig. 6 the images of bare CNR128 disk and of CNR128 disks coated with different chitosan-GDL formulations before and after the corrosion tests are shown.

The occurrence of corrosion processes was clearly observed in the bare disk, used as reference. In the case of bronze disks coated with pure chitosan and chitosan/glycerol the corrosion treatments affect the coating transparency and removability and also lead to the modification of the alloy substrate appearance after film removal. In fact, SEM analysis (Fig. S5) puts on evidence the presence of coating residues after removal. Indeed, it cannot be discarded some extent of polymer degradation under the test conditions, and it might explain the change in appearance of alloy substrates and the incomplete removal of the protective coating. To address this issue, pure chitosan coating was investigated also by FT-IR spectroscopy before and after the accelerated corrosion test (Fig. 7). The small peak at  $880\text{ cm}^{-1}$ , corresponding to wagging (the CH bending out of the plane of the ring) of the saccharide structure of chitosan [45,46], disappears after the thermal treatment with HCl vapours, thus supporting the hypothesis of polymer degradation probably due to the hydrolysis of the pyranose ring catalysed by the acidic environment.

Nevertheless, it was observed that the pure chitosan film have protective effect to some extent, since the formation of corrosion products was not detected on the alloy substrates after film removal compared with the bare disk used as reference (see SEM images in Supporting Information, Fig. S5).

Noticeably, in the case of inhibitors-containing coatings the films remain completely transparent (Fig. 6), they can be easily removed from the substrate disks after the treatment and, more importantly, the alloy substrates remain unaltered. These evidences demonstrate that the presence of inhibitors prevents modifications both of the coating and of the alloy substrates. As shown in Figs. 8 and 9, chitosan/inhibitor films from GDL maintain their homogeneity after the corrosion test. SEM images, at low magnification, clearly show the occurrence of degradation processes in the bare alloy (Fig. 8a) and the absence of

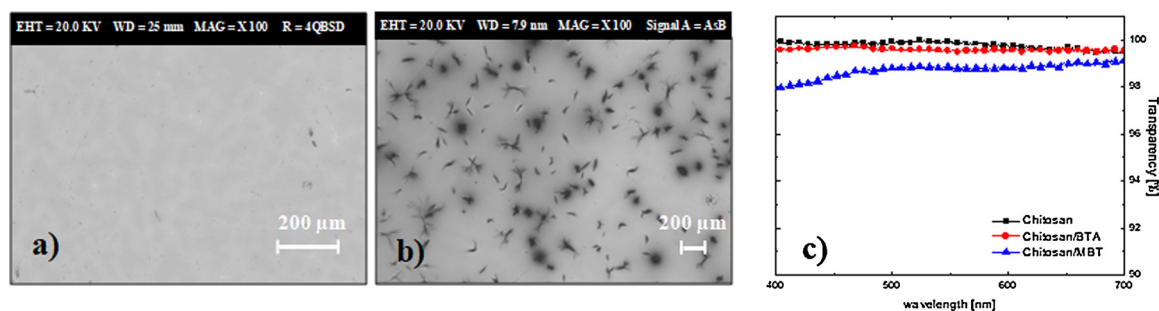


Fig. 5. SEM images of chitosan films prepared from GDL solutions with the addition of a) BTA and b) MBT corrosion inhibitor deposited on alloy CNR128 substrates. (c) Transparency percentage of coatings prepared from GDL solutions deposited on glass slides: chitosan (black squares), chitosan/BTA (blue triangles), chitosan/MBT (red circles). (For interpretation of the references to colour in this figure legend, the reader is referred to the web version of this article.)

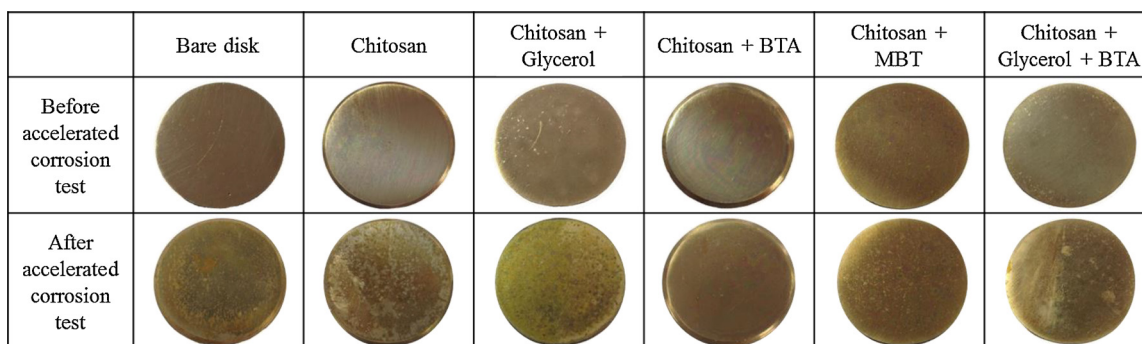


Fig. 6. Photographs of bare CNR128 disk and CNR128 disks coated with different chitosan-GDL formulations before and after the accelerated corrosion test at 50 °C for 1 h.

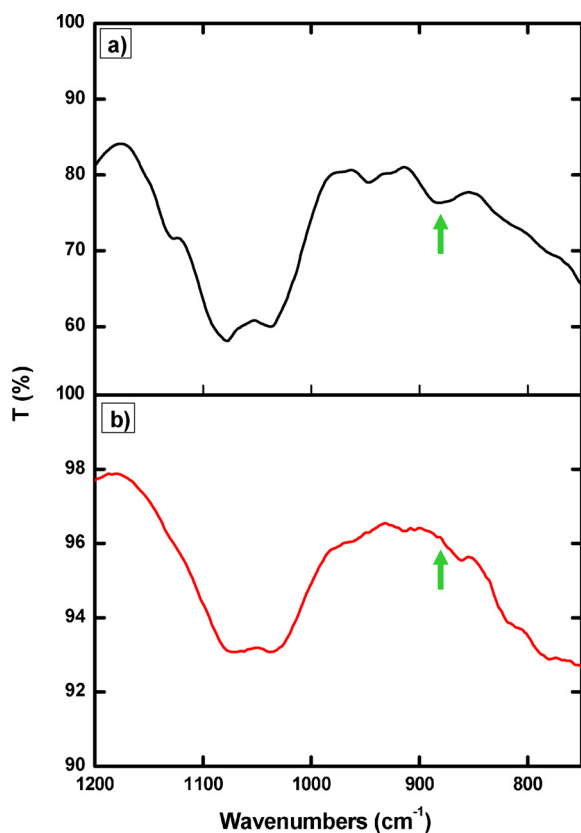


Fig. 7. FTIR spectra of bronze alloy coated with chitosan film prepared by GDL before a), and after b) thermal treatment (1 h, 50 °C) with acid vapours.

damages onto the coated alloy surfaces (Fig. 8b and c).

The SEM images of chitosan-inhibitor coatings, in Fig. 9, were recorded near the area where the films were removed after the corrosion

treatments, thus showing that the alloy morphology does not undergo significant modifications. EDS analysis on the alloy surfaces after film removal also confirm the absence of corrosion products and species containing chloride after exposition to acid vapours (Fig. S6). These findings reveal that even low amounts of BTA and MBT (0.05 wt.% with respect to chitosan solution) embedded in chitosan films are able to inhibit the formation of corrosion products on bronze alloys and to stabilize the polymer matrix, thus avoiding the loss of film transparency and giving to the coating a complete removability.

The efficiency of chitosan-BTA coatings from GDL in the presence of glycerol was also evaluated. In spite of the presence of the inhibitor, a loss of film transparency was observed (Fig. 6) when glycerol is added to the formulation. The use of a hydrophilic plasticizer, such as glycerol, even if it has a positive effect on the film quality, does not improve the coating appearance after the corrosion tests, probably because it increases the ability of the film to retain water, thus decreasing its stability. It is known [47] that the addition of glycerol results in a higher hydrophilicity of the chitosan films, which is attributable to the hygroscopicity of glycerol [48]. Moreover, plasticizers improve the flexibility and extensibility of the film by decreasing the intermolecular interaction of polymer chains and increasing their mobility. This is useful to prevent the cracking of the film, but also increases the permeability to gases and vapours [49,50].

On the basis of these findings, chitosan/inhibitor coatings without glycerol result the most interesting and promising for the corrosion protection of bronze works of art and will be further investigated.

Since chitosan-based coatings are proposed for the conservation of indoor artefacts, conventional electrochemical measurements with immersion in water solutions cannot be used to quantify their protective efficacy since they would cause coating dissolution. Then, the protective efficacy of the coatings was investigated by means of accelerated corrosion treatments in the presence of aggressive species, able to promote degradation processes and rapidly provide information. In order to quantify the ability of coatings to prevent degradation processes, an image analysis protocol has been exploited.

The protective efficacy of chitosan/inhibitor coatings prepared from

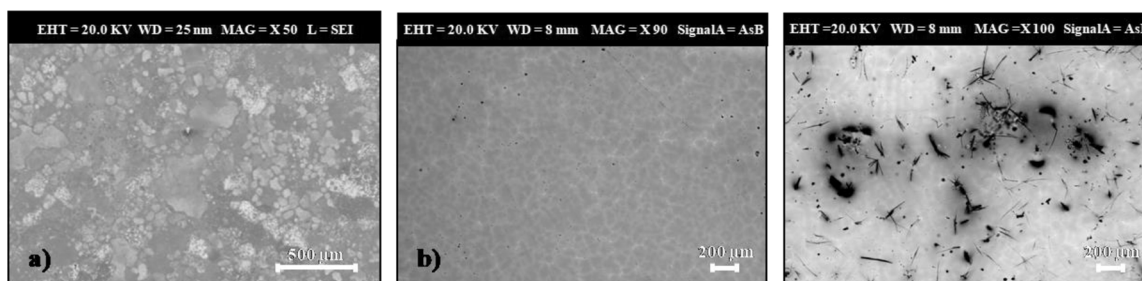


Fig. 8. SEM images of a) alloy CNR128 bare substrate and substrates coated with b) chitosan/BTA and c) chitosan/MBT films from GDL solutions after thermal treatment (1 h, 50 °C) with acid vapours.

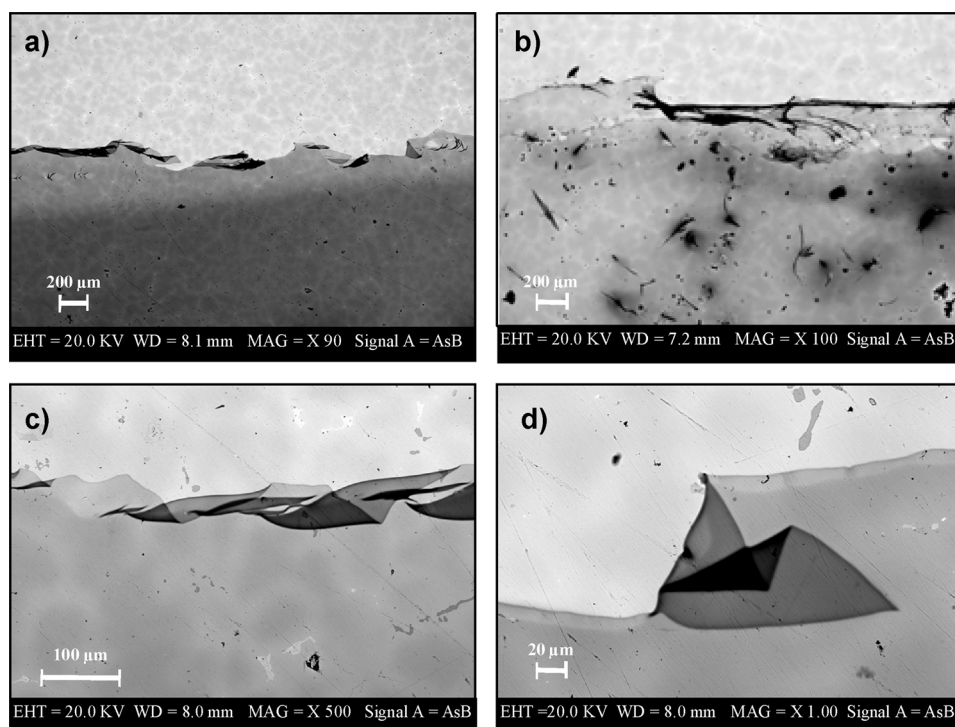


Fig. 9. SEM images of alloy CNR128 substrates coated with a) chitosan/BTA and b) chitosan/MBT films from GDL solutions after thermal treatment (1 h, 50 °C) with acid vapours. In the images the boundary between the film and the alloy bare after film removal can be appreciated. c), d) Magnifications of the image reported in part a).

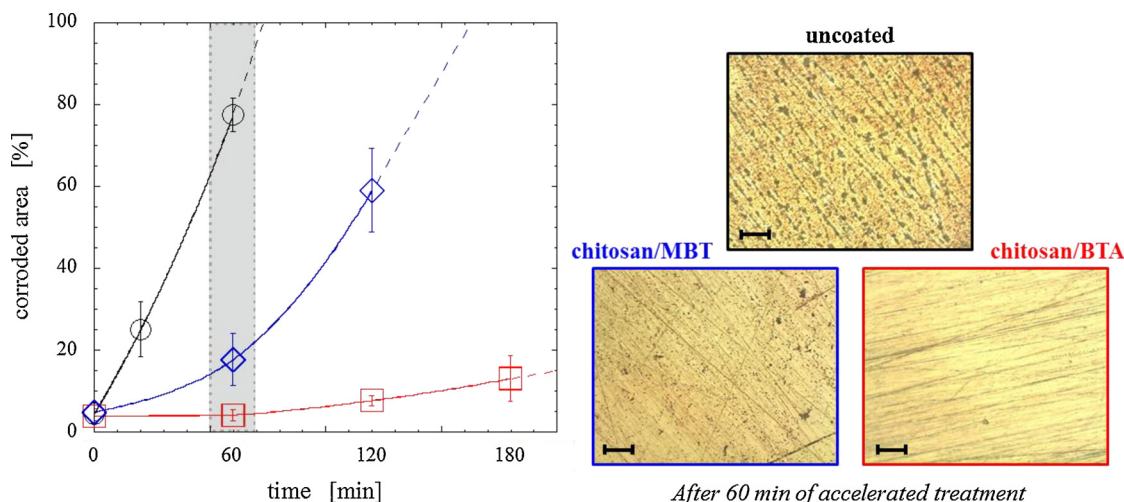


Fig. 10. Percentage of corroded surface calculated by image analysis as a function of the duration of accelerated corrosion treatments: uncoated bronze disk (black circles), disks covered with chitosan/BTA (red squares) and chitosan/MBT coatings (blue diamonds). Representative optical images of the alloy surface after accelerated corrosion treatments for 60 min are reported on the right. From top to bottom: uncoated bronze disk, disks covered with chitosan/BTA and chitosan/MBT coatings. Scale bars correspond to 10 μm. (For interpretation of the references to colour in this figure legend, the reader is referred to the web version of this article.)

GDL solutions was further investigated by prolonging the accelerated corrosion treatments and observing the occurrence of surface modifications at different time intervals by optical microscopy. The results of the image analysis, performed to estimate the percentage of corroded surface, are reported in Fig. 10 for the chitosan/BTA and chitosan/MBT coatings. The uncoated alloy disk was used as reference system.

The obtained results confirm that chitosan/inhibitor coatings noticeably protect the bronze surface from corrosion and their efficacy is much more pronounced in the presence of BTA. In particular, after 1 h of accelerated corrosion treatment the surface bare alloy is almost totally corroded (corroded surface  $\approx$  80%), whereas less than 20% and 5% of surface is corroded in the presence of chitosan/MBT and chitosan/BTA coatings, respectively. When prolonging the accelerated corrosion treatments, significant differences in the protective efficacy of the two coatings emerge. Indeed, chitosan/BTA coating is able to

protect the metal surface even after 3 h, whereas for the disk coated with chitosan/MBT more than 50% of surface is corroded after 2 h. The main reason of such difference can be ascribed to the different protective efficacy of corrosion inhibitors. The results in Fig. 10 suggest that chitosan/inhibitor coatings, in particular chitosan/BTA formulation, are promising systems for a reliable protection of copper-based alloys and the image analysis can be successfully applied for the quantification of the performances of protective systems.

More insights into the protective properties of chitosan/inhibitor coatings were achieved by comparison with their single components. In order to evaluate if there is a merely additive effect, inhibitor and polymer matrix were also deposited on the metal substrate by using a two-step deposition procedure. The photographs in Figs. 6 and 11 clearly show that chitosan/inhibitor coating is able to prevent modifications in surface appearance after corrosion treatments and has a



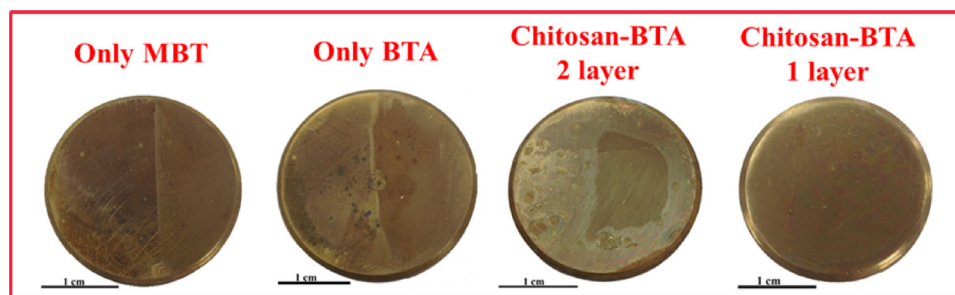


Fig. 11. Photographs of CNR128 disks coated with only MBT, only BTA, chitosan-BTA prepared by a two-step deposition and chitosan-BTA obtained by a one-step procedure after the accelerated corrosion treatments. In the images of only MBT and only BTA are visible both the film (left half) and the alloy bare after film removal (right half).

higher protective efficacy with respect to the same amount of pure inhibitor or pure chitosan coating. Moreover, the coating consisting of a first layer of pure inhibitor and a second layer of pure chitosan has a significantly lower stability and transparency than the mixed chitosan/inhibitor coating, thus suggesting the existence of a synergic effect between chitosan and corrosion inhibitor on the protection of copper-based alloy (Fig. 11).

The polymer matrix probably acts as an inhibitor reservoir and also contributes to the formation of a barrier layer, thus improving the protective properties. Differently from pure chitosan coatings, no changes in the FTIR spectra of chitosan-inhibitor coatings were observed around  $880\text{ cm}^{-1}$  after thermal treatments with acid vapours (Fig. S7). This result suggests that the presence of the inhibitor may avoid polymer degradation and enhance the coating removability after the accelerated corrosion test.

Moreover, the high affinity between inhibitors and alloy [52,53] plays a key role in the protective action, and it has been confirmed by FTIR measurements, since after film removal the spectrum of the alloy substrates show signals which can be attributed to the inhibitors (spectra reported in Fig. S8). These peaks are not detectable in the chitosan-inhibitor coatings, suggesting that their protective efficacy can be ascribed to the migration of inhibitor molecules towards the alloy surface and the formation of a protective inhibitor layer at polymer-alloy interface [51,52]. This behaviour could be relevant in thin films and makes them promising for the conservation of works of art.

### 3.4. Requirements for applications on works of art

Protective coatings for works of art have to satisfy specific requirements, such as transparency, removability and protective efficacy. To easily appreciate the aesthetic properties of chitosan-based coatings, the developed formulations were tested using an alloy substrate with a shiny surface finish. The results of the transparency measurements, removability tests and corrosion treatments suggest that chitosan-inhibitor coatings are able to preserve the aesthetic properties of the metal substrate, can be completely removed without any residues and prevent the alloy degradation.

Moreover, these new formulations are more sustainable and safe than commercial products typically used for the conservation of bronze works of art. For example, the products based on BTA dispersed in acrylic resins are applied and removed using harmful organic solvents and the inhibitor content is about the 0.3 wt/vol%. The chitosan coatings can be applied and removed from water/ethanol solutions and the inhibitor content is the 0.05 wt/vol%, thus representing a promising alternative to commercial products for an effective and safe conservation.

## 4. Conclusions

The protective efficacy of chitosan-based coatings to hinder degradation processes in copper alloy substrates was investigated for applications in cultural heritage conservation. During the optimization of the formulations the effect of the type of acid used for chitosan

dissolution has been investigated and the results reveal its key role on the morphology of the deposited chitosan coating and on its interaction with the copper-based alloy. In particular, the use of GDL leads to high quality chitosan films, since it does not induce the formation of Pb-based platelets, which were detected in the presence of AcOH. Moreover, the incorporation of BTA and MBT in the chitosan-based coatings improves their quality, anticorrosion properties and removability, due to a synergic effect between the polymer matrix and the corrosion inhibitors.

The results of the image analysis, exploited to quantify the protective efficacy, confirm that the developed chitosan coatings with both BTA and MBT are effective in the corrosion inhibition, in particular superior performance can be achieved with BTA. All these findings make chitosan-based coatings very promising for their application in the sustainable, long lasting and safe protection of bronze works of art stored or exhibited in indoor environment.

### Funding sources

The work has been carried out within the NANORESTART project funded by the European Union's Horizon 2020 research and innovation programme under the grant agreement No 646063.

### Acknowledgements

The authors thank A. Aldi and F. Docimo for the technical support in the experiments.

### Appendix A. Supplementary data

Supplementary data associated with this article can be found, in the online version, at <https://doi.org/10.1016/j.porgcoat.2018.05.002>.

### References

- [1] R.L. Quirino, T.F. Garrison, M.R. Kessler, Matrices from vegetable oils, cashew nut shell liquid, and other relevant systems for biocomposite applications, *Green Chem.* 16 (2014) 1700–1715.
- [2] D. Watkinson, Shreir's corrosion, 4th ed., Preservation of Metallic Cultural Heritage vol. 4, Elsevier, London, 2010, pp. 3307–3340.
- [3] M. Finšgar, I. Milošev, Inhibition of copper corrosion by 1,2,3-benzotriazole: a review, *Corros. Sci.* 52 (2010) 2737–2749.
- [4] D.A. Pillard, J.S. Cornell, D.L. Dufresne, M.T. Hernandez, Toxicity of benzotriazole and benzotriazole derivatives to three aquatic species, *Water Res.* 35 (2001) 557–560.
- [5] Health Council of the Netherlands, 1,2,3-Benzotriazole. Health-Based Recommended Occupational Exposure Limit, (2000).
- [6] C. Peniche, W. Arguelles-Monal, F.M. Goyocolea, Monomers, Polymers and Composites from Renewable Resources, 1st ed., Elsevier, Amsterdam, 2008, pp. 517–542.
- [7] Y. Wang, C. Dong, D. Zhang, P. Ren, L. Li, X. Li, Preparation and characterization of a chitosan-based low pH-sensitive intelligent corrosion inhibitor, *Int. J. Miner. Metall. Mater.* 22 (9) (2015) 998–1004.
- [8] J. Carneiro, J. Tedim, S.C.M. Fernandes, C.S.R. Freire, A. Gandini, M.G.S. Ferreira, M.L. Zheludkevich, Functionalized chitosan-based coatings for active corrosion protection, *Surf. Coat. Technol.* 226 (2013) 51–59.
- [9] B. Ghosh, M.W. Urban, Self-repairing oxetane-substituted chitosan polyurethane networks, *Science* 323 (2009) 1458–1460.
- [10] A. Lutz, O. Van den Berg, J. Van Damme, K. Verheyen, E. Bauters, I. De Graeve,



- F.E. Du Prez, H. Terryn, A shape-recovery polymer coating for the corrosion protection of metallic surfaces, *Appl. Mater. Interfaces* 7 (2015) 175–183.
- [11] J. Tedim, S.K. Poznyak, A. Kuznestova, D. Raps, T. Hack, M.L. Zheludkevich, M.S.G. Ferreira, Enhancement of active corrosion protection via combination of inhibitor-loaded nanocontainers, *Appl. Mater. Interfaces* 2 (2010) 1528–1535.
- [12] A. Domard, M. Domard, D. Severian, M. Decker (Eds.), *Polymeric Biomaterials*, 2001, pp. 187–212 New York. Chapter 9.
- [13] M.N.V. Ravi Kumar, A review of chitin and chitosan applications, *React. Funct. Polym.* 46 (2000) 1–27.
- [14] F.J. Pavinatto, L. Caseli, O.N. Oliveira, Chitosan in nanostructured thin films, *Biomacromolecules* 11 (2010) 1897–1908.
- [15] M.Z. Elabee, E.S. Abdou, Chitosan based edible films and coatings: a review, *Mater. Sci. Eng. C* 33 (2013) 1819–1841.
- [16] A. Curulli, G. Di Carlo, G.M. Ingo, C. Riccucci, D. Zane, C. Bianchini, Chitosan stabilized gold nanoparticle-modified Au electrodes for the determination of polyphenol index in wines: a preliminary study, *Electroanalysis* 24 (2012) 897–904.
- [17] M.A. Garcia, M.N. Martino, N.E. Zanitzky, Microstructural characterization of plasticized starch-based films, *Starch* 52 (2000) 118–124.
- [18] J. Zhang, C. Dai, Z. Wen, J. Wei, Study on the effect of the coating thickness on corrosion behavior of AZ91D magnesium alloy in m-SBF, *Int. J. Electrochem. Sci.* 10 (2015) 6002–6013.
- [19] M. Fekry, A.A. Ghoneim, M.A. Ameer, Electrochemical impedance spectroscopy of chitosan coated magnesium alloys in a synthetic sweat medium, *Surf. Coat. Technol.* 238 (2014) 126–132.
- [20] L. de Y. Pozzo, T.F. da Conceição, A. Spinelli, N. Scharnagl, A.T.N. Pires, Chitosan coatings crosslinked with genipin for corrosion protection of AZ31 magnesium alloy sheets, *Carbohydr. Polym.* 181 (2018) 71–77.
- [21] F. Gebhardt, S. Seuss, M.C. Turhan, H. Hornberger, S. Virtanen, A.R. Boccaccini, Characterization of electrophoretic chitosan coatings on stainless steel, *Mater. Lett.* 66 (2012) 302–304.
- [22] J. Carneiro, J. Tedim, S.C.M. Fernandes, C.S.R. Freire, A.J.D. Silvestre, A. Gandini, M.G.S. Ferreira, M.L. Zheludkevich, Chitosan-based self-healing protective coatings doped with cerium nitrate for corrosion protection of aluminum alloy 2024, *Prog. Org. Coat.* 75 (2012) 8–13.
- [23] J. Carneiro, J. Tedim, S.C.M. Fernandes, C.S.R. Freire, A. Gandini, M.G.S. Ferreira, M.L. Zheludkevich, Chitosan as a smart coating for controller release of corrosion inhibitor 2-mercaptobenzothiazole, *ECS Electrochem. Lett.* 2 (6) (2013) C19–C22.
- [24] M.N. El-Haddad, Chitosan as a green inhibitor for copper corrosion in acidic medium, *Int. J. Biol. Macromol.* 55 (2013) 142–149.
- [25] M.M. Antonijevic, S.M. Milic, M.B. Petrovic, Films formed on copper surface in chloride media in the presence of azoles, *Corros. Sci.* 51 (2009) 1228–1237.
- [26] D.A. Winkler, M.A. Breedon, E. Hughes, F.R. Burden, A.S. Barnard, T.G. Harvey, I. Cole, Towards chromate-free corrosion inhibitors: structure–property models for organic alternatives, *Green Chem.* 16 (2014) 3349–3357.
- [27] E. Stupnišek-Lisac, A. Lončarić Božić, Cafuk, I. Low-toxicity copper corrosion inhibitors, *Corrosion* 54 (1998) 713–720.
- [28] E. Abdullayev, V. Abbasov, A. Tursunbyeva, V. Portnov, H. Ibrahimov, G. Mukhtarova, Y. Lvov, Self-healing coatings based on halloysite clay polymer composites for protection of copper alloys, *Appl. Mater. Interfaces* 5 (2013) 4464–4471.
- [29] F. Faraldi, B. Cortese, D. Caschera, G. Di Carlo, C. Riccucci, T. De Caro, G.M. Ingo, Smart conservation methodology for the preservation of copper-based objects against the hazardous corrosion, *Thin Solid Films* 622 (2017) 130–135.
- [30] G.M. Ingo, M.P. Casaletto, T. De Caro, C. Riccucci, Production of reference ancient Cu-based alloys and their accelerated degradation methods, *Appl. Phys. A: Mater. Sci. Process* 83 (2006) 617–622.
- [31] G.M. Ingo, E. Angelini, G. Bultrini, I. Calliari, M. Dabalà, T. De Caro, Study of long-term corrosion layers grown on high-tin leaded bronzes by means of the combined use of GDOES and SEM + EDS, *Surf. Interface Anal.* 34 (2002) 337–342.
- [32] C.K.S. Pillai, W. Paul, C.P. Sharma, Chitin and chitosan polymers: chemistry: solubility and fiber formation, *Prog. Polym. Sci.* 34 (2009) 641–678.
- [33] K. Kurita, Chitin and chitosan: functional biopolymers from marine crustaceans, *Mar. Biotechnol.* 8 (3) (2006) 203–226.
- [34] J.W. Park, K.H. Choi, Acid-base equilibria and related properties of chitosan, *Bull. Korean Chem. Soc.* 4 (1983) 68–71.
- [35] M. Rinaudo, G. Pavlov, J. Desbrieres, Influence of acetic acid concentration on the solubilization of chitosan, *Polymer* 40 (1999) 7029–7032.
- [36] M. Rinaudo, G. Pavlov, J. Desbrieres, Solubilization of chitosan in strong acid medium, *Int. J. Polym. Anal. Charact.* 5 (1999) 267–276.
- [37] K.M. Kim, J.H. Son, S.K. Kim, C.L. Weller, M.A. Hanna, Properties of chitosan films as a function of pH and solvent type, *J. Food Sci.* 71 (2006) E119–124.
- [38] D.A. Scott, Bronze disease: a review of some chemical problems and the role of relative humidity, *J. Am. Inst. Conserv.* 29 (1990) 193–206.
- [39] D.M. Bastidas, M. Criado, S. Fajardo, V.M. La Iglesia, E. Cano, J.M. Bastidas, Copper deterioration: causes: diagnosis and risk minimisation, *Int. Mater. Rev.* 55 (2010) 99–127.
- [40] G.M. Ingo, T. De Caro, C. Riccucci, E. Angelini, S. Grassini, S. Balbi, P. Bernardini, D. Salvi, L. Bousselmi, A. Cilingiroglu, M. Gener, V.K. Gouda, O. Al Jarrah, S. Khosroff, Z. Mahdjoub, Z. Al Saad, W. El-Saddik, P. Vassiliou, Large scale investigation of chemical composition, structure and corrosion mechanism of bronze archeological artefacts from Mediterranean basin, *Appl. Phys. A* 83 (4) (2006) 513–520.
- [41] D. Prat, A. Wells, J. Hayler, H. Sneddon, C.R. McElroy, S. Abou-Shehadad, P.J. Dunne, Selection guide of classical- and less classical-solvents, *Green Chem.* 18 (2016) 288–296.
- [42] Y. Shchipunov, N. Ivanova, V. Silant'ev, Bionanocomposites formed by *in situ* charged chitosan with clay, *Green Chem.* 11 (2009) 1758–1761.
- [43] Y. Shchipunov, S. Sarin, I. Kim, C.S. Ha, Hydrogels formed through regulated self-organization of gradually charging chitosan in solution of xanthan, *Green Chem.* 12 (2010) 1187–1195.
- [44] K. Catali, J. Santillán, Q. Williams, A high-pressure infrared spectroscopic study of PbCO<sub>3</sub>-cerussite: constraints on the structure of the post-aragonite phase, *Phys. Chem. Miner.* 32 (2005) 412–417.
- [45] Q. Yuan, J. Shah, S. Hein, R.D. Misra, *Acta Biomater.* 6 (2010) 1140–1148.
- [46] M.F. Queiroz, K.R. Teodosio Melo, D.A. Sabry, G.L. Sasaki, H.A. Oliveira Rocha, *Mar. Drugs* 13 (2015) 141–158.
- [47] J.L. Chen, Y. Zhao, Effect of molecular weight, acid, and plasticizer on the physicochemical and antibacterial properties of  $\beta$ -chitosan based films, *J. Food Sci.* 77 (5) (2012) E127–136.
- [48] M. Lavorgna, F. Piscitelli, P. Mangiacapra, G. Buonocore, Study of the combined effect of both clay and glycerol plasticizer on the properties of chitosan films, *Carbohydr. Polym.* 82 (2) (2010) 291–298.
- [49] N.E. Suyatma, L. Tighzert, A. Copinet, Effects of hydrophilic plasticizers on mechanical, thermal, and surface properties of chitosan films, *J. Agric. Food Chem.* 53 (2005) 3950–3957.
- [50] N. Gontard, S. Guilbert, J.L. Cuq, Water and glycerol as plasticizers affect mechanical and water vapor barrier properties of an edible wheat gluten film, *J. Food Sci.* 58 (1993) 206–211.
- [51] N. Kovacevic, I. Milosev, A. Kokalj, The roles of mercapto, benzene: and methyl groups in the corrosion inhibition of imidazoles on copper: II. Inhibitor-copper bonding, *Corros. Sci.* 98 (2015) 457–470.
- [52] I. Milosev, N. Kovacevic, J. Kovac, A. Kokalj, The roles of mercapto, benzene, and methyl groups in the corrosion inhibition of imidazoles on copper: I. Experimental characterization, *Corros. Sci.* 98 (2015) 107–118.